Evaluation and measurement of forces between two conducting spheres

A. Corona Cruz
Facultad de Ciencias Físico Matemáticas, Benemérita Universidad Autónoma de Puebla,
Apartado Postal 1152, 72001 Puebla Pue., México
e-mail: acorona@fcfm.buap.mx

E. Ley-Koo
Instituto de Física, Universidad Nacional Autónoma de México.
Apartado Postal 20-364, 01000 México, D. F. México
e–mail: eleykoo@fisica.unam.mx

Recibido el 28 de febrero de 2002; aceptado el 25 de junio de 2002

The forces between pairs of conducting spheres at different separations and with fixed potential differences are evaluated using bispherical coordinates on the basis of Ref. 1. The experimental arrangement, the method and the results of the measurement of such forces are reported. The analysis of the measurements is carried out by comparison with the forces evaluated for the corresponding values of the geometrical and electrical parameters, finding a good agreement.

Keywords: Conducting spheres; electrostatic force.

Se evalúan las fuerzas entre pares de esferas conductoras a diferentes separaciones y con diferencias de potencial fijas, usando coordenadas biesféricas con base en la Ref. 1. Se reportan el arreglo experimental, el método y los resultados de la medición de tales fuerzas. El análisis de las mediciones se realiza comparando con las fuerzas evaluadas para los valores correspondientes de los parámetros geométricos y eléctricos, mostrándose un buen acuerdo.

Descriptores: Esferas conductoras; fuerza electrostática.

PACS: 41.10 Dq

1. Introduction

This didactic article is aimed at both students and teachers of advanced undergraduate or graduate courses of electromagnetism. The references "On the evaluation of the capacitance of bispherical capacitors" [1], Forces between two uniformly charged cylinders versus forces between two conducting cylinders" [2], and "Measurement of forces between two parallel conducting cylinders" [3] provide the mathematical, physical and experimental background of the problem studied in the present article.

The work deals with the forces between pairs of conducting spheres at different separations and with fixed potential differences. The evaluation of such forces is developed in Sec. 2 on the basis of the work of Góngora and Ley Koo, using bispherical coordinates for the description of the associated electric field [1]. The experimental arrangement, the method of measurement, and the data on the geometrical, electrical and force variables are reported in Sec. 3, including a comparison with the forces evaluated according to the results of the previous section. Section 4 contains a discussion of the above results, as well as other points of didactic interest. The Appendix presents the key equations of [1] needed for the development of Sec. 2.

2. Evaluation of the forces from the electric field described in bispherical coordinates

The evaluation to be developed in this section on the basis of Ref. 1 had already been anticipated in Ref. 2. Both articles deal with the same electrostatic problems of two conductors kept at a fixed potential difference, but differ in the geometry of the conductors, namely spherical and cylindrical, respectively. In Ref. 2 the cylindrical geometry was chosen because of its simple solution and corresponding didactic value; the experimental work for the measurement of the forces between pairs of cylinders at a fixed potential difference and different separations has also been done [3]. In Ref. 2 it was also recognized that the solution for the spherical geometry based on Ref. 1 could also be constructed, but requires some elaborate mathematics. Next we provide the details of such a construction, using some equations of Ref. 1 as presented in the Appendix.

We assume that one of the spherical conductors defined by $\eta = \eta_1$ is kept at an electrical potential V_1 while the other defined by $\eta = \eta_2$ is grounded. The electrical force on either one is evaluated by integrating the Maxwell stress tensor

$$\overleftrightarrow{T} = \frac{\vec{E}\vec{E}}{4\pi} - \overleftrightarrow{I}\,\frac{\vec{E}\cdot\vec{E}}{8\pi} \tag{1}$$

over its area,

$$\vec{F} = \oint d\vec{a}\cdot\overleftrightarrow{T} = \oint d\vec{a}\cdot\left[\frac{\vec{E}\vec{E}}{4\pi} - \overleftrightarrow{I}\,\frac{\vec{E}\cdot\vec{E}}{8\pi}\right]. \tag{2}$$

In the case of conductors both the area elements and the electric intensity field are perpendicular to the surface. Consequently, the contribution of the second term in Eq. (2) is a half of that of the first term. Specifically, the force on the grounded conductor is evaluated by using the electric field intensity from Eq. (A.10) and the unit vector $\hat{\eta}$ from Eq. (A.3), obtaining

$$\vec{F} = \frac{1}{8\pi}\oint d\vec{a}\cdot\vec{E}\vec{E} = \frac{1}{8\pi}\int_0^{\pi}\int_0^{2\pi} h_\xi d\xi h_\varphi d\varphi E\vec{E}$$
$$= \frac{1}{8\pi}\left(\frac{V_1}{a}\right)^2 \sum_{l=0}^{\infty}\frac{(l+\frac{1}{2})C_l(\cosh\ \eta_1)}{\sinh[(l+\frac{1}{2})(\eta_1-\eta_2)]}\sum_{l'=0}^{\infty}\frac{(l'+\frac{1}{2})C_{l'}(\cosh\ \eta_1)}{\sinh[(l'+\frac{1}{2})(\eta_1-\eta_2)]}$$
$$\times\, a^2\int_0^{\pi}\int_0^{2\pi} d\xi\sin\xi d\varphi[-\sinh\eta_2\sin\xi(\hat{i}\cos\varphi+\hat{j}\sin\varphi)-\hat{k}(\cosh\ \eta_2\cos\xi-1)]N_1P_l(\cos\xi)N_{l'}P_{l'}(\cos\xi). \quad (3)$$

In the evaluation of this integral it can be pointed out that the product of the scale factors $h_\xi h_\varphi$, Eqs. (A.2), the unit vector $\hat{\eta}_2$, Eq. (A.3), and the factors $(\cos h\eta_2-\cos\xi)^{3/2}$ of the electric intensity field, Eq. (A.10), leads to the cancelation of the binomial factors. The integration over the azimuthal angle gives zero for the terms in the transverse directions $\hat{i}$ and $\hat{j}$, and 2π for the longitudinal term along $\hat{k}$. The remaining integrations over ξ for the two terms in the binomial multiplying $\hat{k}$ correspond to the matrix element of cosξ,

$$\int_0^{\pi} d\xi\sin\xi N_lP_l(\cos\xi)\cos\xi N_{l'}P_{l'}(\cos\xi)$$
$$= \frac{(l+1)}{\sqrt{(2l+1)(2l+3)}}\delta_{l+1,l'}$$
$$+\frac{l}{\sqrt{(2l-1)(2l+1)}}\delta_{l-1,l'}, \quad (4)$$

and the orthonormality integral

$$\int_0^{\pi} d\xi\sin\xi N_lP_l(\cos\xi)N_{l'}P_{l'}(\cos\xi)=\delta_{l,l'}. \quad (5)$$

The final result is

$$\vec{F}_2 = \hat{k}\frac{V_1^2}{4}\sum_{l=0}^{\infty}\frac{C_l(\cosh\ \eta_1)(l+\frac{1}{2})}{\sinh[(l+\frac{1}{2})(\eta_1-\eta_2)]}$$
$$\times\left\{\frac{C_l(\cosh\ \eta_1)(l+\frac{1}{2})}{\sinh[(l+\frac{1}{2})(\eta_1-\eta_2)]}\right.$$
$$-\cosh\ \eta_2\left[\frac{C_{l+1}(\cosh\ \eta_1)(l+\frac{3}{2})}{\sinh(l+\frac{3}{2})(\eta_1-\eta_2)]}\frac{l+1}{\sqrt{(2l+1)(2l+3)}}\right.$$
$$\left.\left.+\frac{C_{l-1}(\cosh\eta_1)(l-\frac{1}{2})}{\sinh[(l-\frac{1}{2})(\eta_1-\eta_2)]}\frac{l}{\sqrt{(2l-1)(2l+1)}}\right]\right\}. \quad (6)$$

Since the force is proportional to the square of the potential difference it is convenient to use the reduced force F/V^2. Its value depends only on the coordintes η_1 and η_2 of each sphere, which are determined by the geometrical parameters $R_1,\ R_2$ and d through Eqs. (A.4) and (A.6). Its experimental value can be determined from measurements with different values of the potential difference.

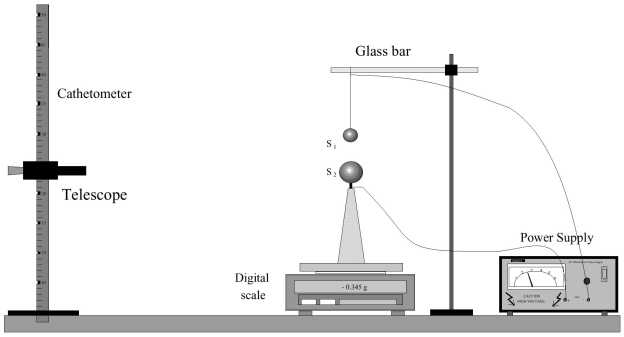

FIGURE 1. Experimental arrangement to measure the forces between conducting spheres.

3. Measurement of the forces and comparison with their calculated values

The experimental arrangement for measuring the electrical forces between conducting spheres, maintained at fixed potential differences, involved electrical, aligning and force measuring instrumentations, as sketched in Fig. 1 and described next. A PASCO ES-9070 Kilovolt power Supply with an output varying from 0 to 6 Kilovolts provided the potential difference between the conducting copper spheres. A cathetometer, with a length of 50 cm and an accuracy of $\pm$ 0.001 cm, was used to establish the vertical alignment of the spheres and to measure their separation. An Ohaus 300D electronic balance, with a capacity of 30 g, an accuracy of $\pm$0.001 g and a reproducibility of $\pm$ 0.007 g, was used to measure the electrostatic force between the spheres.

Some of the details about the geometrical, electrical and mechanical arrangements and measurements are also described following the successive steps of the experiment. Spheres with different combinations of diameters $2R$ = 1.775, 1.111, 0.952, and 0.873 cm were used. One of the spheres was hung from a horizontal glass rod using a thin # 32 copper wire; the other sphere is supported by a 20 cm high dielectric base resting on the plate of the balance (Fig. 1). The upper and lower spheres are connected to the positive and negative terminals of the power supply, respectively, using # 32 copper wires. The voltage applied to the spheres was measured with a high voltage tip coupled to a Fluke 79 digital multimeter; the chosen values were V = 7.5, 10.9, 14.2, 17.5 and 20.5 statvolts. The balance was placed on a concrete base in order to eliminate any vibrations,

and it had a servomechanism to keep its plate fixed. The vertical alignment between the upper sphere and the lower one was checked with the axis of the cathetometer's lens. The error for misalignment was estimated to be of the order of $\pm$ 0.01 cm. The cathetometer was used to measure the closest distance Δ between the upper and lower spheres, leading to the distance $d = \Delta + R_1 + R_2$ between their respective centres. Before the voltage is applied to the spheres, the reading of the balance is adjusted to zero, 0.000 g; after the voltage V is applied by turning on the power supply, the attraction between the spheres produces a negative reading M in grams. The numerical value of the force of attraction in dynes is obtained as the product of this reading times the local value of the acceleration of gravity, g = 978 cm/s^2 for Puebla City. If the spheres are not properly aligned, the upper sphere moves and the balance reading oscillates. When the alignment is achieved, the upper sphere remains at rest and the balance reading is stable after a situation of electromechanical equilibrium is reached. This provides a criterion about the quality of the alignment. Each time it was satisfied, the reading of the balance and the separation between the spheres Δ indicated by the cathetometer's vernier were written down. The separation between the spheres was systematically changed by raising the upper sphere.

The numerical results of the measured geometrical, electrical and force parameters are reported in Table I and Figs. 2-3 , including the comparison with the theoretical values for the reduced force F_t/V^2 from Eq. (6). The first three sets of measurements involve pairs of spheres with different radii and the same value of the potential difference, and they are presented graphically in Figs. 2a-c. The last two sets of measurements correspond to a pair of spheres with the same radii $R_1 = R_2 = 1.775$ for two different values of the potential difference, and are incorporated in Figs. 3a and 3b.

The theoretical formula of Eq. (6) is an infinite series, but its fast convergence has been numerically tested. For the first four sets of data in Table I, two or three terms are sufficient to achieve convergence of the evaluated forces to the reported accuracy. For the last set of data the number of terms had to be increased to 5-10 as the separation between the spheres Δ became smaller from 0.22 to 0.02 cm.

The numerical comparison of the measured and evaluated values of the reduced forces, as reported in the last two columns of Table I and their graphical representations in Figs. 2 and 3, show their overall good agreement for spheres of different sizes at different distances and different potential differences.

The last two sets of data for $V = 20.5$ and 3.75 statvolts cover the large and small separation domains, respectively. The continuous smooth increasing variation of the reduced force as the separation decreases can be followed in the Table I. Notice the different scales for the reduced force in Figs. 3a and 3b, which are necessary in order to appreciate the changes in the respective domains. For very small separations the voltage was reduced in order to avoid the discharge between the spheres.

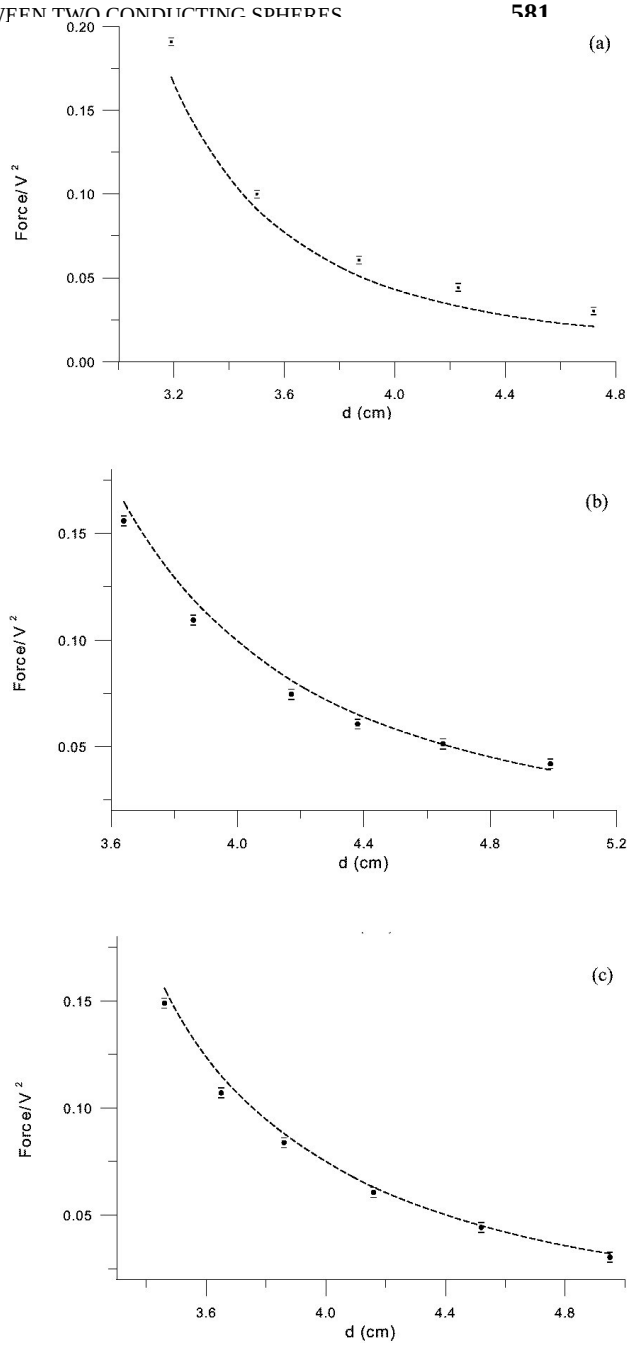

FIGURE 2. Reduced force versus distance for pairs of spheres with radii a) $R_1 = 1.775$cm, $R_2 = 0.873$cm, b) $R_1 = 1.775$cm, $R_2 = 0.952$ and c) $R_1 = 1.775$cm, $R_2 = 1.111$cm. Experimental values in circles with error bars and theoretical values from Eq. (6) in broken-line curves.

4. Discussion

The evaluation of the forces between conducting spheres at given separations and potential differences has been discussed in Sec. 2. The corresponding method and numerical results of measurement of the geometrical, electrical and force parameters have been reported in Sec. 3, including a comparison with the values of the reduced force evaluated on

TABLE I. Numerical values of the radii of the spheres R_1 and R_2 (cm), the potential difference V (statvolts), distance between their centers *d*(cm), reading of the balance *M* (g) and corresponding force *F* (dynes), measured reduced force F/V^2, and its counterpart evaluated from Eq. (6) F_t/V^2 ((dynes/statvolts)^2).

R_1	R_2	V	d	M	F	F/V^2	F_t/V^2
1.775	0.873	20.5	4.72	13	13	0.031 ± 0.001	0.021
			4.23	19	19	0.045 ± 0.003	0.033
			3.87	26	25	0.59 ± 0.004	0.051
			3.50	43	42	0.100 ± 0.005	0.091
			3.19	82	80	0.190 ± 0.008	0.170
1.775	0.952	20.5	4.95	13	13	0.031 ± 0.003	0.032
			4.52	19	18	0.043 ± 0.004	0.045
			4.16	26	25	0.059 ± 0.004	0.063
			3.86	36	35	0.083 ± 0.005	0.088
			3.65	46	45	0.107 ± 0.005	0.115
			3.46	64	63	0.150 ± 0.007	0.156
1.775	1.111	20.5	4.99	18	18	0.043 ± 0.004	0.039
			4.65	22	21	0.050 ± 0.004	0.051
			4.38	26	25	0.059 ± 0.004	0.065
			4.17	32	31	0.074 ± 0.004	0.081
			3.86	47	46	0.109 ± 0.005	0.119
			3.64	67	65	0.155 ± 0.007	0.165
1.775	1.775	20.5	8.30	7	7	0.017 ± 0.003	0.012
			7.40	9	9	0.021 ± 0.003	0.18
			6.61	13	13	0.031 ± 0.003	0.027
			5.95	20	20	0.047 ± 0.004	0.041
			5.44	28	27	0.064 ± 0.004	0.060
			5.07	38	37	0.088 ± 0.005	0.083
			4.80	47	46	0.109 ± 0.005	0.110
			4.50	67	65	0.155 ± 0.007	0.159
			4.33	86	84	0.200 ± 0.008	0.206
			4.20	108	106	0.252 ± 0.009	0.259
1.775	1.775	3.75	4.26	3	3	0.21 ± 0.08	0.23
			3.77	12	12	0.8 ± 0.02	0.90
			3.67	30	29	2.1 ± 0.4	1.73
			3.63	46	45	3.2 ± 0.6	2.64
			3.62	56	55	3.9 ± 0.7	3.0
			3.59	87	85	6 ± 1	5.4
			3.58	190	186	13 ± 2	7.25
			3.57	241	236	17 ± 3	10.9

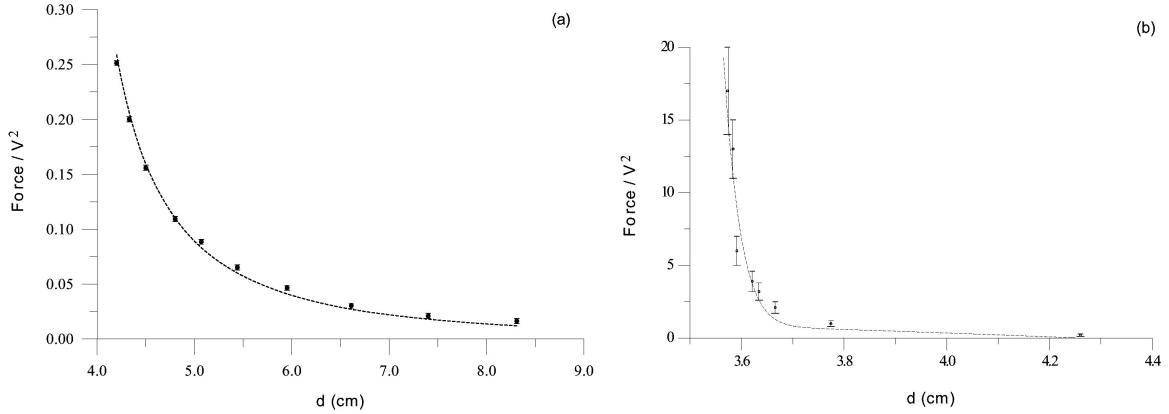

FIGURE 3. Reduced force versus distance for a pair of spheres with equal radii $R_1 = 1.775$ cm for large and small separations.

the basis of Eq. (6). A good agreement between the experimental and theoretical values was found.

Some general and some specific points of didactic interest are worth pointing out. The problem of the forces between two conductors involves geometrical and electrical elements. In the cases of Refs. 2 and 3 and this work, the choices of coordinates allow the simultaneous incorporation of both elements in the formulation and solution of the problem. For the cylindrical conductors the lowest harmonic term in bipolar coordinates gives the exact solution to the problem [2]. For the spherical conductors, the use of bispherical coordinates leads to the $R-$ separable harmonic expansion of the electrostatic potential of Eq. (A.7), which in turn generates the electric intensity field of Eq. (A.10), and this is the basis for obtaining Eqs. (3)-(6) for the force between the spheres. The fast convergence of the latter is an indication that it has indeed incorporated both the geometrical and electrical elements in the right combination. As a point of comparison, the solution based on the infinite set of charge images on both spheres, obtained by Maxwell [3], involves a much more slowly convergent series.

The original question "Under what conditions can the force between two conducting spheres be approximated by Coulomb's law?" which motivated our writing of Refs. 2 and 3 and the present article, was already answered in Ref. 2. Here it can be taken up again emphasizing that the inverse square law is valid for point charges or for uniformly charged spheres, *ie*, monopole-monopole interaction. The charge distributions in the conducting spheres studied in the present work are given by Eq. (A.12) and its counterpart for $\eta = \eta_1$. Figures 4 illustrate the charge distributions on the surfaces of a) a pair of sphere with the same radii $R_1 = R_2 = 1.775$ cm and b) two spheres with very different radii $R_1 = 1.775$ and $R_2 = 0.01$ cm, respectively, as functions of the ξ bispherical coordinate and the separation distance d. Their departures from uniform distributions reflect the importance of the electrostatic induction effect, and translate into deviations from Coulomb's force.

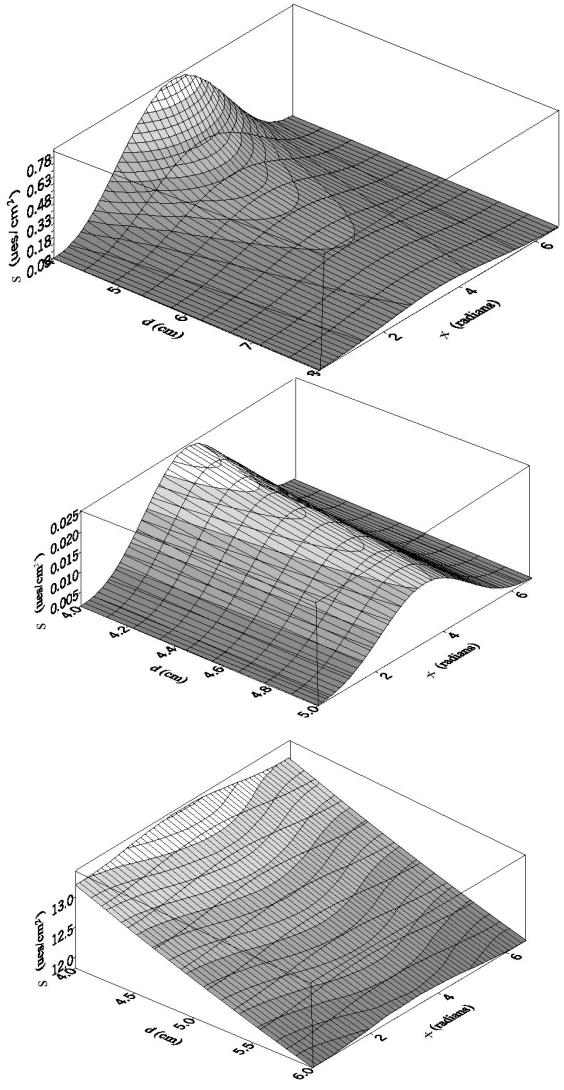

(b)

FIGURE 4 a) Surface distributions $\sigma(d, \xi)$ for a pair of spheres with equal radii $R_1 = R_2 = 1.775$ cm. b) Two spheres with different radii $R_1 = 1.775$ cm and $R_2 = 0.01$ cm as functions of the bispherical coordinate and separation distance d.

A Appendix

The transformation equations between bispherical and cartesian coordinates are

$$x = \frac{a\sin\xi\cos\varphi}{\cosh\,\eta-\cos\xi}, y = \frac{a\sin\xi\sin\varphi}{\cosh\,\eta-\cos\xi},$$
$$z = \frac{a\sinh\eta}{\cosh\,\eta-\cos\xi}. \qquad \text{(A.1)}$$

The scale factors and unit vectors in biespherical coordinates are given by ,

$$h_\xi = h_\eta = \frac{a}{\cosh\,\eta-\cos\xi},$$
$$h_\varphi = \frac{a\sin\xi}{\cosh\,\eta-\cos\xi}, \qquad \text{(A.2)}$$

and

$$\hat{\xi} = \frac{(\cosh\,\eta\cos\xi-1)(i\cos\varphi+\hat{j}\sin\varphi)-\hat{k}\sinh\,\eta\sin\xi}{\cosh\,\eta-\cos\xi}$$
$$\hat{\eta} = -\frac{\sinh\,\eta\sin\xi(\hat{i}\cos\varphi+\hat{j}\sin\varphi)+\hat{k}(\cosh\,\eta\cos\xi-1)}{\cosh\,\eta-\cos\xi},$$
$$\hat{\varphi} = -\hat{i}\sin\varphi+\hat{j}\cos\varphi \qquad \text{(A.3)}$$

The positions of the conducting spheres are defined by the respective values of the coordinate $\eta=\eta_1>0$ and $\eta=\eta_2<0$ with the corresponding radii

$$R_1 = a\text{csch}\,\eta_1,$$
$$R_2 = -a\text{csch}\,\eta_2, \qquad \text{(A.4)}$$

and centres on the z-axis at ,

$$z_1 = a\coth\eta_1,$$
$$z_2 = a\coth\eta_2. \qquad \text{(A.5)}$$

The spheres become points in the limiting situations $\eta_1\to\infty$ and $\eta_2\to-\infty$ for which the radii of Eq. (A.4) vanish and $z_1\to a, z_2\to -a$ in Eq. (A.5); these points are the so-called poles. The distance between the poles for the spheres described by Eqs. (A.4)and (A.5) can be written in terms of the radii and the distance between the centres of the spheres d as

$$2a = \frac{\sqrt{(d+R_1+R_2)(d+R_1-R_2)(d-R_1-R_2)(d-R_1+R_2)}}{d}. \qquad \text{(A.6)}$$

The electrostatic potential function between the spherical conductors $\eta=\eta_1$ at a potential V_1 and $\eta=\eta_2$ connected to the ground is given by the biespherical harmonic expansion

$$\phi(\xi,\eta,\varphi) = V_1(\cosh\,\eta-\cos\xi)^{1/2}\sum_{l=0}^{\infty}\frac{C_l(\cosh\,\eta_1)}{\sinh\,[(l+\frac{1}{2})(\eta_1-\eta_2)]}\sinh\,[(l+\frac{1}{2})(\eta-\eta_2)]N_lP_l(\cos\xi), \qquad \text{(A.7)}$$

where

$$C_l(cosh\,\eta_1) = \int_0^\pi \frac{\sin\xi' N_lP_l(\cos\xi')d\xi'}{(cosh\,\eta_1-\cos\xi')^{\frac{1}{2}}},$$
$$= \frac{1}{2^lN_l}(sech\,\eta_1)^{\frac{1}{2}+l}$$
$$\times\,{}_2F_1(\frac{l}{2}+\frac{1}{4},\frac{l}{2}+\frac{3}{4};l+\frac{3}{2};sech^2\eta_1) \qquad \text{(A.8)}$$

are the coefficients in the normalized Legendre polynomial expansion of the inverse square root of the binomial

$$\frac{1}{(\cosh\eta_1-\cos\xi)^{\frac{1}{2}}} = \sum_{l=0}^{\infty}C_l(\cosh\eta_1)N_lP_l(\cos\xi). \qquad \text{(A.9)}$$

The reader may notice the presence of the binomial in Eq. (A.7), which is a reflection of the $R-$ separability of the Laplace equation. It is also easy to verify that the potential function satisfies the boundary condition at the respective electrodes.

The electric intensity field is obtained as the negative gradient of Eq. (A.7):

$$\vec{E}(\xi,\eta,\varphi) = -\left[\hat{\xi}\frac{\partial}{h_\xi \partial\xi} + \hat{\eta}\frac{\partial}{h_\eta \partial\eta} + \hat{\varphi}\frac{\partial}{h_\varphi \partial\varphi}\right]\phi(\xi,\eta,\varphi)$$

$$= -\frac{V_1}{a}(\cosh\eta - \cos\xi)^{\frac{3}{2}} \sum_{l=0}^{\infty} \frac{C_l(\cosh\eta_1)}{\sinh\left[(l+\frac{1}{2})(\eta_1-\eta_2)\right]} \left\{\hat{\xi}\left[N_l \frac{dP_l(\cos\xi)}{d\xi} + \frac{\sin\xi}{2(\cosh\eta - \cos\xi)} N_l P_l(\cos\xi)\right]\right.$$

$$\left.\times \sinh\left[(l+\frac{1}{2})(\eta-\eta_2)\right] + \hat{\eta}\left[(l+\frac{1}{2})\cosh\left[(l+\frac{1}{2})(\eta-\eta_2)\right] + \frac{\sinh\,\eta \sinh\left[(l+\frac{1}{2})(\eta-\eta_2)\right]}{2(\cosh\,\eta - \cos\xi)}\right] N_l P_l(\cos\xi)\right\}. \quad \text{(A.10)}$$

In particular, on the grounded spherical conductor it becomes

$$\vec{E}(\xi,\eta=\eta_2,\varphi) = -\hat{\eta}\frac{V_1}{a}(\cosh\eta_2 - \cos\xi)^{\frac{3}{2}}$$

$$\times \sum_{l=0}^{\infty} \frac{C_l(\cosh\eta_1)(l+\frac{1}{2})}{\sinh\left[(l+\frac{1}{2})(\eta_1-\eta_2)\right]} N_l P_l(\cos\xi), \quad \text{(A.11)}$$

which is perpendicular to the spherical surface. The same holds at the other electrode.

The electric charge distribution on the grounded sphere follows from Gauss's law,

$$\sigma(\xi,\eta=\eta_2,\varphi) = \frac{\hat{\eta}\cdot\vec{E}(\xi,\eta=\eta_2,\varphi)}{4\pi}$$

$$= -\frac{V_1}{4\pi a}(\cosh\eta_2 - \cos\xi)^{\frac{3}{2}}$$

$$\times \sum_{l=0}^{\infty} \frac{C_l(\cosh\eta_1)(l+\frac{1}{2})}{\sinh\left[(l+\frac{1}{2})(\eta_1-\eta_2)\right]} N_l P_l(\cos\xi) \quad \text{(A.12)}$$

The total charge on the sphere is obtained by integrating Eq. (A.12) over its surface,

$$Q_2 = \int_0^{\pi}\int_0^{2\pi} \sigma(\xi,\eta,\varphi) h_\xi d\xi h_\varphi d\varphi\Big|_{\eta=\eta_2}$$

$$= -\frac{V_1}{4\pi a} 2\pi a^2 \sum_{l=0}^{\infty} \frac{C_l(\cosh\eta_1)(l+\frac{1}{2})}{\sinh\left[(l+\frac{1}{2})(\eta_1-\eta_2)\right]}$$

$$\times \int_0^{\pi} \frac{d\xi \sin\xi N_l P_l(\cos\xi)}{(\cosh\eta_2 - \cos\xi)^{\frac{1}{2}}}$$

$$= -\frac{V_1}{2} a \sum_{l=0}^{\infty} \frac{(l+\frac{1}{2}) C_l(\cosh\eta_1) C_l(\cosh\eta_2)}{\sinh\left[(l+\frac{1}{2})(\eta_1-\eta_2)\right]}. \quad \text{(A.13)}$$

1. T. Góngora and E. Ley Koo, *Rev. Mex. Fis.* **42** (1996) 663.
2. E. Ley Koo and G. Monsivais, *Rev. Mex. Fis.* **41** (1995) 610; E. Ley Koo and G. Monsivais, *Rev. Mex. Fis.* **45** (1999) 108.
3. A. Corona Cruz and E. Ley Koo, *Rev. Mex. Fís.* **48** (2002) 485.
4. J. C. Maxwell, *A Treatise on Electricity and Magnetism*, Vol. 1 (Dover, New York, 1954), pp. 266-273.